C.P. No. 296
(17,573)
A.R.C. Technical Report

C.P. No. 296
(17,573)
A.R.C. Technical Report

MINISTRY OF SUPPLY

AERONAUTICAL RESEARCH COUNCIL
CURRENT PAPERS

Compressor Cascade Flutter Tests Part II. 40° Camber Blades, Low and Medium Stagger Cascades

By

D. A. Kilpatrick and J. Ritchie

LONDON . HER MAJESTY'S STATIONERY OFFICE
1956
THREE SHILLINGS NET

C.P. No. 296

U.D.C. No. 533.695.5: 621.438.031.3

Report No.R.163

October, 1954.

NATIONAL GAS TURBINE ESTABLISHMENT

Compressor cascade flutter tests
Part II
40° camber blades, low and medium stagger cascades

- by -

D. A. Kilpatrick

and

J. Ritchie

SUMMARY

The tests reported here continue the cascade flutter investigation at N.G.T.E., the first part of which, already reported, deals with 20° camber blades, medium and high stagger cascades. In agreement with those test results, three main flutter zones, of high stress, are detected, viz. stalling flutter, shock-stalling flutter and choking flutter. Their disposition, with reference to the aerodynamic cascade characteristics, is also in general agreement.

Good correlation of stalling flutter with the experimentally determined blade force derivative with respect to incidence, is obtained, but only incomplete correlation of shock-stalling and choking flutter with the blade force derivative with respect to Mach number.

CONTENTS

ILLUSTRATIONS

1.0 Introduction

To increase the available amount of data relevant to the problem of blade flutter in the axial-flow compressor, an investigation into cascade blade flutter characteristics is being undertaken at N.G.T.E. A Report has already been issued (Reference 1) dealing with the results from 20° camber blades, in medium and high stagger cascades. This present Report extends the comprehensive investigations to 40° camber blades, in low and medium stagger cascades. Preliminary results on the low stagger, 40° camber cascade have already been given (Reference 2). All these cascades are of 10C4 sections, with circular arc camber lines, blade aspect ratio of 3.0 and pitch/chord ratio of 1.0.

2.0 Description of tests

2.1 Cascade details

The test blades were made in steel S.1 and their method of construction is indicated in Figure 1, the blade forms being machined from S.1 strip and then brazed into a root platform of mild steel as shown in Section AA. This method of construction was used to ensure high blade profile accuracy and material consistency as well as being convenient for the assembly of different stagger cascades. The blade material damping, as manifested by decrement measurements of free vibration in the fundamental cantilever mode, is higher than that for the cast blades which were used for the tests of Reference 1, but is reasonably consistent. Two methods of assembling the blades in cascade were used. Initially the blades were brazed together at the roots as shown in Figure 1(a). Later, to improve the accuracy of assembly and also to facilitate replacement of broken blades, the "plate-mounting" method of Figure 1(b) was adopted, the blades' root platforms being drilled, tapped and screwed to a base plate; the gap between the blades is then shimmed and soldered, care being taken to "tin" all surfaces adequately.

Both types of cascade tested were made up of blades of section 10C4/40C50, chord 0.75 in. and aspect ratio 3.0. The low stagger cascade was set at a stagger of -24.5° and the medium stagger cascade at -34.9°.

2.2 Test techniques

The movement of the tip of one of the blades when installed in the N.G.T.E. No.6 High Speed Cascade Tunnel and when oscillating in the air stream, is recorded optically by means of light reflected from a small mirror in the blade tip at 20 per cent chord from the leading edge. The recording is made on moving-film, and the analysis of the record yields blade vibration frequency, blade alternating stress and also the change in the "mean" blade tip position (which gives a measure of the mean aerodynamic force on the blade).

Test runs were made at fixed air incidences, recordings of the blade flutter and the relevant total head and static pressures being made at suitable increments of inlet air speed. The procedure was thus similar to that described more fully in Reference 1. Typical blade tip movement records are shown in Figure 2.

3.0 Test results

The cascades were tested over a wide range of incidence and Mach number. The increments of tunnel setting angle were 1° and the incidence range of the tests on the low stagger cascade was -8° to $+20^\circ$ approximately, that for the medium stagger cascade being -6.5° to $+16.5^\circ$ approximately. The maximum incidence attainable is restricted by the cascade tunnel geometry and is thus lower for the medium than for the low stagger cascade.

Flutter of the cascade blades was seen to occur at almost all incidences and was of significant amplitude over a large part of the incidence range. This severe flutter was noted to occur at speeds above the critical Mach number M_{nc}, defined for the purposes of these tests as that Mach number at which the pressure rise through the cascade, $\Delta P/(P_{tot} - P_{stat.})$, begins to fall. This is thus in agreement with the results reported in Reference 1.

The flutter observed was mainly of the fundamental (1st) cantilever mode, and caused alternating stresses of as much as ±30 tons/in.^{2} In addition to this fundamental mode there occurred a certain amount of 2nd cantilever mode vibration and also, for the medium stagger cascade, a more complex "diagonal" mode, confined to a small region at negative incidence. The stresses for the 2nd cantilever mode were mostly very small (less than ±2 tons/in.^{2}) reaching, at certain conditions, peak values of ±5.5 tons/in.^{2}. In the case of the "diagonal" mode (medium stagger cascade only) the stresses reached quite high values, viz. ±17 tons/in.^{2}. All the stresses quoted are root stresses, being derived from the recordings of blade tip movement (at the mirror location), with the aid of laboratory calibrations under controlled excitation conditions. The "peak" stresses are the maximum stresses as recorded (during the exposure time of about 2 or 3 seconds per condition), while the "mean" stresses are a visual estimate only from the same record.

3.1 Low stagger cascade

The blades of this cascade are, in standard notation, 10C4/40C50 set at a stagger angle of -24.5°, and assembled into cascade by the root-brazing method of Figure 1(a). Two separate cascades were necessary to complete the test range, the natural frequencies of both cascades lying between 500 and 520 c.p.s., and with an average logarithmic decrement of 0.025. The tip clearance was 0.050 in.

3.1.1 Blade stresses

Plotted in Figure 3 are the maximum alternating blade stresses against Mach number for given air inlet angles. The stresses are seen to be generally more severe and extensive at the higher incidences, reaching a peak of approximately ±30 tons/in.^{2} ; (the ultimate tensile strength of this steel is about 35 tons/in.^{2}). Figure 4 shows the recorded stresses plotted as contours on a base of inlet Mach number and air angle, together with the curves of critical Mach number and maximum Mach number M_{nm}, as evaluated from measurements during the flutter tests. The maximum Mach number is defined as that at which the pressure rise through the cascade becomes zero.

In agreement with the tests of Reference 1, it is seen that severe flutter occurs in three main regions, viz. <u>shock-stalling</u> flutter just above the critical Mach number and from about 46° to 49° air inlet angle;

stalling flutter above the critical Mach number and from 53° inlet angle upwards; and choking flutter, which occurs mainly above the maximum Mach number, extending over almost the whole of the positive incidence range. The onset of the stalling flutter is seen to occur almost precisely at the stalling incidence, as indicated by the peak of the "force" against incidence curves of Figure 5(b).

The inlet angle (47°) marked as i_s (th.) in Figure 4 is the theoretical stalling air inlet angle as evaluated using the data sheets presented in Reference 3. This theoretical stalling incidence is, however, based upon the use of the drag coefficient and this fact (as well as the basic inaccuracies of the evaluation) probably accounts for the discrepancy between the inlet angle equivalent to i_s (th.) and the stalling air inlet angle as indicated by the peak of the experimentally determined force versus incidence curves.

This particular cascade form is one on which two previous preliminary tests have been performed, the first of which is reported in Reference 2. These other tests used cascades of cast blades (H.R. crown Max.), of somewhat less accurate form and stagger etc than the steel strip blades of this Report, and were much more restricted in range. It is interesting to compare the results of the three sets of tests and Figure 6 shows a comparison of their contours of stress greater than ±10 tons/in.² It will be noted that the general agreement is good. An unexplained discrepancy at the onset of the stalling flutter regions is, however, observed in which stalling flutter for one of the cast cascades "intrudes" below its critical Mach number curve. The delay in the fall of its critical Mach number with the inlet angle, in this region, is probably associated with this blade vibration.

3.1.2 Blade aerodynamic forces

By measuring the "mean" displacement of the blade tip for each condition, a measure of the mean aerodynamic force, F, on the blade can be obtained (Section 2.2). A selection of the resulting curves of force F against Mach number is plotted in Figure 5(a) and of force against inlet angle in Figure 5(b), the ordinates being scaled in tip displacement, to which F is proportional.

It will be noted that the curves of Figure 5(b) especially for the lower Mach numbers, do not particularly resemble the usual two-dimensional C_L curves. This is probably due to the influence of secondary flows etc. in the three-dimensional experimentally derived force curves, together with the inaccuracies of measuring very small mean (steady) blade tip movements with (at times) superimposed large oscillating tip movements.

The regions of negative slope of the force versus Mach number curves, $\partial F/\partial M_n < 0$, and of the force versus incidence curves, $\partial F/\partial \alpha_1 < 0$ are plotted on a base of Mach number and air inlet angle together with some of the flutter contours in Figure 7(a). It will be noted that, similar to the findings of Reference 1, there is reasonably good correlation of shock-stalling flutter and $\partial F/\partial M_n < 0$, and between stalling flutter and $\partial F/\partial \alpha_1 < 0$. It should be observed that the negative slope regions as plotted comprise all values of negative $\partial F/\partial M_n$ and $\partial F/\partial \alpha_1$ and take no account of the magnitude of the slope. Inspection of the curves of Figure 5(b) reveals the stalling air inlet angle as being 53°

approximately, at which inlet angle severe stalling flutter begins (Figure 4). There is, however, only very partial correlation between choking flutter and $\partial F/\partial M_n < 0$ for this cascade.

3.2 Medium stagger cascade

This cascade was assembled from blades of form 10C4/40C50 set at a stagger of -34.9°. The first part of the test range was completed using a cascade assembled by the root brazing method of Figure 1(a). The replacement cascade, however, was of the "plate-mounting" type, one blade replacement in this cascade being needed to complete the test range. All the blades concerned were in the frequency range 480 to 500 c.p.s. and with an average logarithmic decrement of 0.020. The tip clearance was 0.050 in. approximately.

3.2.1 Blade stresses

Some of the curves of maximum alternating blade stress against Mach number are plotted in Figure 8, from which it is seen that the fundamental cantilever mode flutter stress reaches a peak of approximately ±30 tons/in.² The 2nd cantilever mode occurs only to a very slight extent, being less than ±4 tons/in.² at all conditions. There is, however, a small region of vibration in a mode of slightly higher frequency than the 2nd cantilever mode, which reaches a maximum stress value of ±17 tons/in.² The nodal pattern for this mode has the same general appearance as the 2nd cantilever mode nodal patterns (see Reference 1 for example) except that the "nodal line" is much more nearly a diagonal line of the blade. This mode is thus referred to as the "diagonal" mode.

In Figure 9 the stresses are plotted as stress contours together with the "oscillatory" critical and maximum Mach numbers. It is seen that the pattern of three main regions of severe flutter is maintained, viz. shock-stalling, choking and stalling flutter. The region of flutter in the "diagonal" mode is distinct but lies mainly within the choking region. Thus, in general, the disposition of the three flutter regions is as before, with the shock-stalling flutter just above critical Mach number and extending from about 54° to 60° air inlet angle, while the choking flutter extends over a wide range of incidence, positive and negative, and lies above the maximum Mach number. Comparison of Figures 9(a) and 9(b) indicates that stalling flutter, in the main, extends from about 63° air inlet angle upwards. The stalling incidence, as indicated by the peak of the force versus incidence curves of Figure 10(b), is also 63°; the theoretical stalling air inlet angle at i_s (th.), being about 57°. The same explanation of this discrepancy as for the low stagger cascade (Section 3.1.1) probably holds. It will be noted that above zero incidence, quite severe flutter occurs throughout the whole region above the critical Mach number.

3.2.2 Blade aerodynamic forces

Figure 10 shows some of the curves of blade mean tip movement plotted against Mach number and against inlet angle. As stated in Section 3.2.1 the major peaks of the force versus incidence curves occur at about 63° air inlet angle, this being equivalent to the stalling incidence and coinciding with the beginning of stalling flutter. To compare regions of negative $\partial F/\partial M_n$ and negative $\partial F/\partial \alpha_1$ with the flutter regions, Figure 7(b) is plotted. If it is remembered that the areas so plotted take no account of the magnitude of the slope of the derivatives $\partial F/\partial M_n$ and $\partial F/\partial \alpha_1$, then it is seen that there is reasonably good correlation between the initial part of stalling flutter and one region of negative $\partial F/\partial \alpha_1$, the other such regions being of lesser magnitude of negative $\partial F/\partial \alpha_1$. There is, though, no real correlation between choking flutter and negative $\partial F/\partial M_n$ and only partial correlation between shock-stalling flutter and negative $\partial F/\partial M_n$.

An interesting phenomenon was observed at very high flows at one or two incidences around the stall point, as exemplified by the force versus Mach number curve for $\alpha_1 = 62.1^\circ$ in Figure 10(a). This shows that the force on the blade at this very high speed condition is unstable and alternates between two widely separated values. Figure 2 reproduces some records obtained under such conditions, from which it will be seen that the changeover from one condition to the other is extremely rapid and is irregular. Similar records were obtained at one or two other nearby incidences. It is thought that this phenomenon is the result of flow detachment and re-attachment as occasioned by shock-wave movements on the blade surface, similar perhaps to the shock-wave development, on cascade blades fixed at both ends, as reported in Reference 4.

4.0 Discussion of results

Three main regions of severe flutter are distinguished from the results of these tests on 40° camber blades, viz.:

(i) Stalling flutter, at incidences above stall.

(ii) Shock-stalling flutter, just above the critical Mach number, and at low incidences.

(iii) Choking flutter, extending over a wide range of incidence and lying mainly above the maximum Mach number.

It is seen that the stresses in these ranges are large and capable of causing blade failure in a very short time. Indeed, in general, almost the whole of the area above the "oscillatory" critical Mach number curve, and especially at positive incidences, is associated with a significant stress level. The differences in the critical Mach numbers as measured under "oscillatory" conditions and as measured with cascade blades fixed at both ends are shown in Figure 6, from which it is noted that the "static" critical Mach number is within "scatter" distance of the three "oscillatory" critical Mach number curves. This indicates that the blade vibration has little effect on the critical Mach number (except in that case where the blade movement is comparatively high). It should here be mentioned that the measurement of the critical Mach number in terms of the pressure rise through the cascade is a less accurate method than the more usual determination of the drag critical Mach number, (as for example in Reference 5).

The correlation of flutter zones with the negative values of the "oscillatory" force derivatives $\partial F/\partial M_n$, as shown in Figure 7, is seen to be reasonably good for the shock-stalling flutter but incomplete for the choking flutter of the low stagger cascade. For the medium stagger cascade, the shock-stalling region and the "diagonal" mode flutter is only partially correlated. Stalling flutter for both cascades occurs almost precisely with regions of negative values of $\partial F/\partial \alpha_1$. Thus it would appear that the use of $\partial F/\partial M_n$ alone as a criterion for choking and shock-stalling flutter is inadequate, although giving good prediction for some conditions. Onset of stalling flutter, however, is well predicted by values of $\partial F/\partial \alpha_1$ sufficiently negative. The simple theory, neglecting damping and phase lag of flow vectors, as presented in Reference 1 gives the condition for self-induced vibration as being when

$$\frac{\partial F}{\partial M_n} \cdot \sin(\alpha_1 - |\zeta|) + \frac{\partial F}{\partial \alpha_1} \frac{\cos(\alpha_1 - |\zeta|)}{M_n} < 0 \qquad ,$$

from which it is apparent that for positive values of $\partial F/\partial M_n$, $\partial F/\partial \alpha_1$ must be less than a certain negative quantity and not merely less than zero to give flutter-prone conditions.

The disposition and type of these flutter regions with reference to the aerodynamic characteristics is similar to the test results of the 20° camber cascade of Reference 1. As stated there, the implications of these cascade flutter tests are that the stalling flutter conditions are difficult to avoid in a high duty compressor operating over a wide speed range, that choking flutter, mainly at negative incidence, might be possible under extreme conditions of compressor operation, and that the shock-stalling flutter condition is close to the nominal design point of some compressor stages and might thus cause trouble at speeds greater than design.

These results together with those reported in Reference 1 are based on cascades of constant aspect ratio, thickness/chord ratio, pitch/chord ratio and on the same base profile, with circular arc camber lines. The characteristics thus determined take no account of these parameters, the effect of variation in which might well alter the magnitude and extent of any flutter. It is, however, felt that the general disposition of the flutter characteristics would be of the same nature.

5.0 Conclusions

This Report presents the results of the second part of the present cascade flutter programme at N.G.T.E., viz. low and medium stagger, medium camber cascades. The three main types of flutter, stalling, shock-stalling and choking flutter as detected in the first part of the investigation (Reference 1) have been detected in these tests. They give rise to stresses high enough to cause early blade failure and their general disposition relative to the aerodynamic characteristics is similar to that of the 20° camber cascade tests.

The tests performed so far have taken no account of the parameters of aspect ratio, thickness/chord ratio, pitch/chord ratio, and the effects of these and other variables require further study. The simple use of the experimentally determined "oscillatory" blade force derivatives, with respect to Mach number and inlet air angle, has been shown to give good flutter correlation for stalling flutter but incomplete correlation of choking and shock-stalling flutter. A more elaborate study of the total blade forces is needed to put this prediction on a quantitative basis.

REFERENCES

No.	Author(s)	Title
1	D. A. Kilpatrick and J. Ritchie	Compressor cascade flutter tests. Part I - 20° camber blades, medium and high stagger cascades. C.P. No. 187. December, 1953.
2	A. D. S. Carter and D. A. Kilpatrick	Preliminary flutter tests on a low stagger compressor cascade. N.G.T.E. Memorandum No. M.141, January, 1952. A.R.C.14629.
3	R. A. Jeffs A. F. Hounsell and R. G. Adams	Further performance data for aerofoils having C.1, C.2 or C.4 base profiles on circular arc camber lines. N.G.T.E. Memorandum No. M.139, December, 1951. A.R.C.14755.
4	K. W. Todd	An experimental study of three-dimensional high speed air conditions in a cascade of axial-flow compressor blades. R. & M. 2792. August, 1948.
5	A. D. S. Carter	Some tests on compressor cascades of related aerofoils having different positions of maximum camber. R. & M. 2694. December, 1948.

FIG. 1.

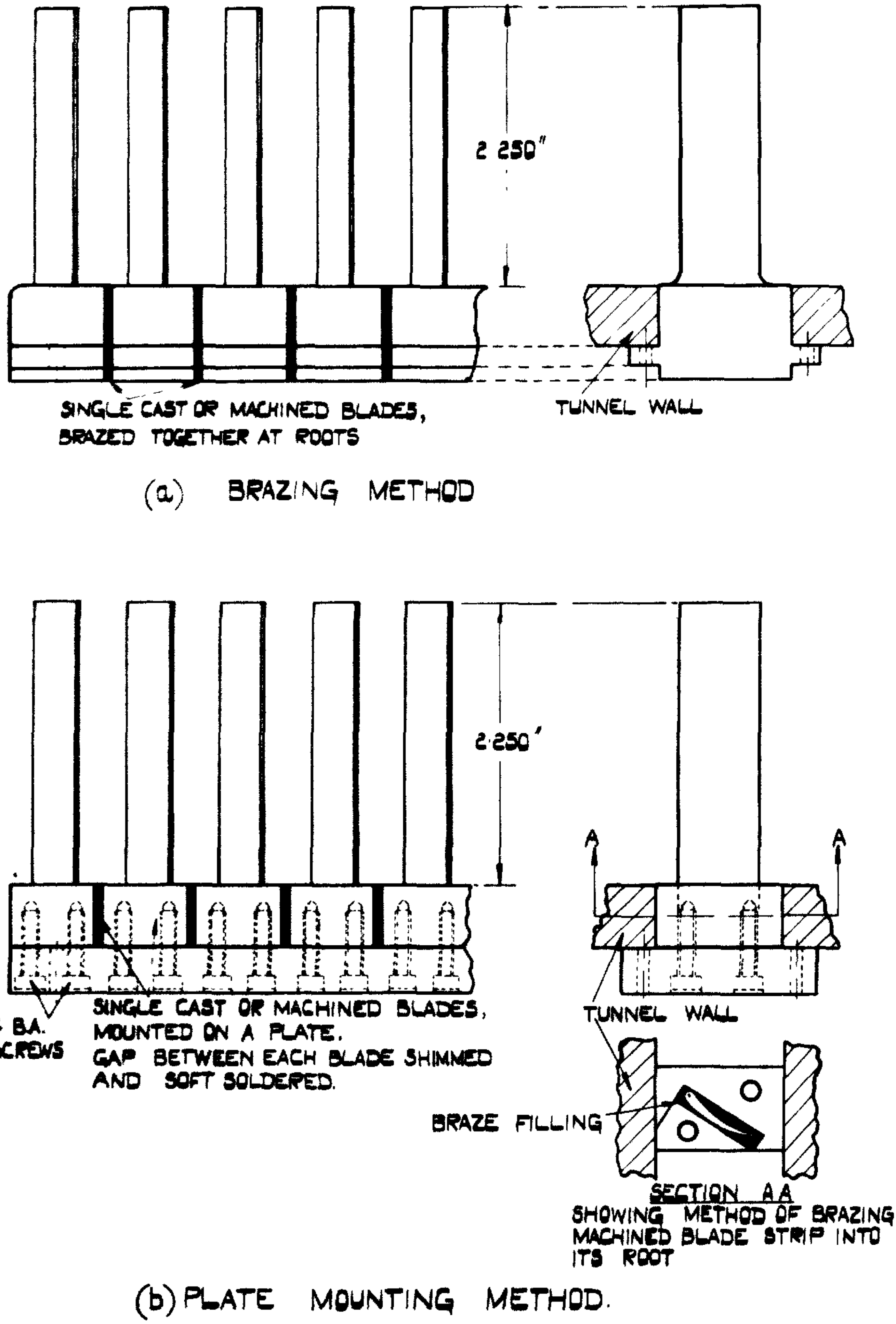

ROOT ATTACHMENT OF BLADES.

FIG. 2.

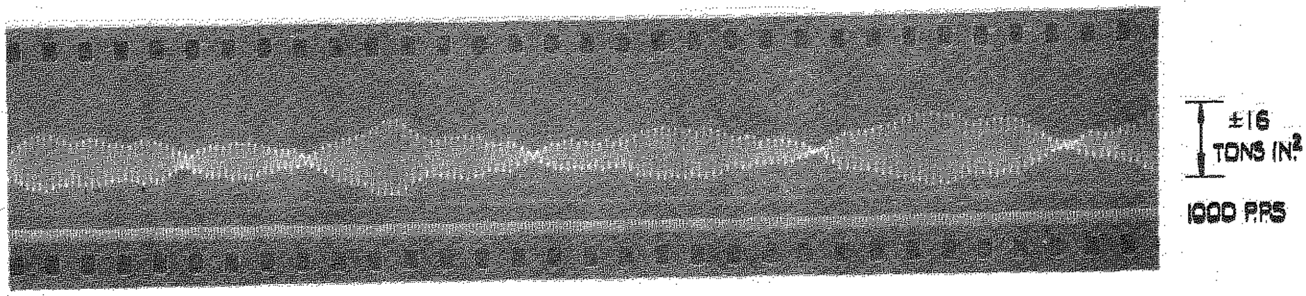

10C4/40C50 $\gamma = -24{\cdot}5^\circ$ $\alpha_1 = 47{\cdot}8^\circ$ $M_n = 0{\cdot}67$
SHOCK STALLING FLUTTER.

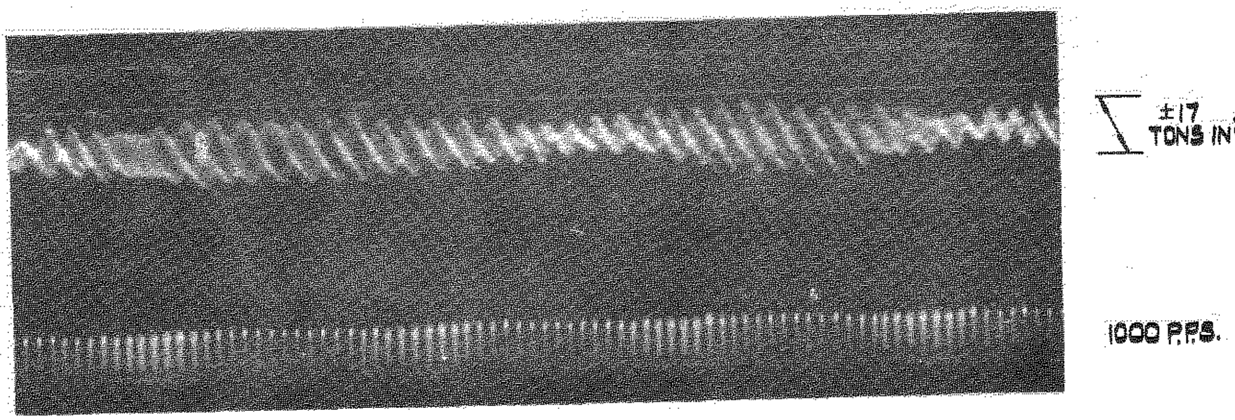

10C4/40C50 $\gamma = -34{\cdot}9^\circ$ $\alpha_1 = 49{\cdot}1^\circ$
'DIAGONAL' MODE, MODULATED BY FUND. CANT. MODE.
(× 3·8 ENLARGEMENT)

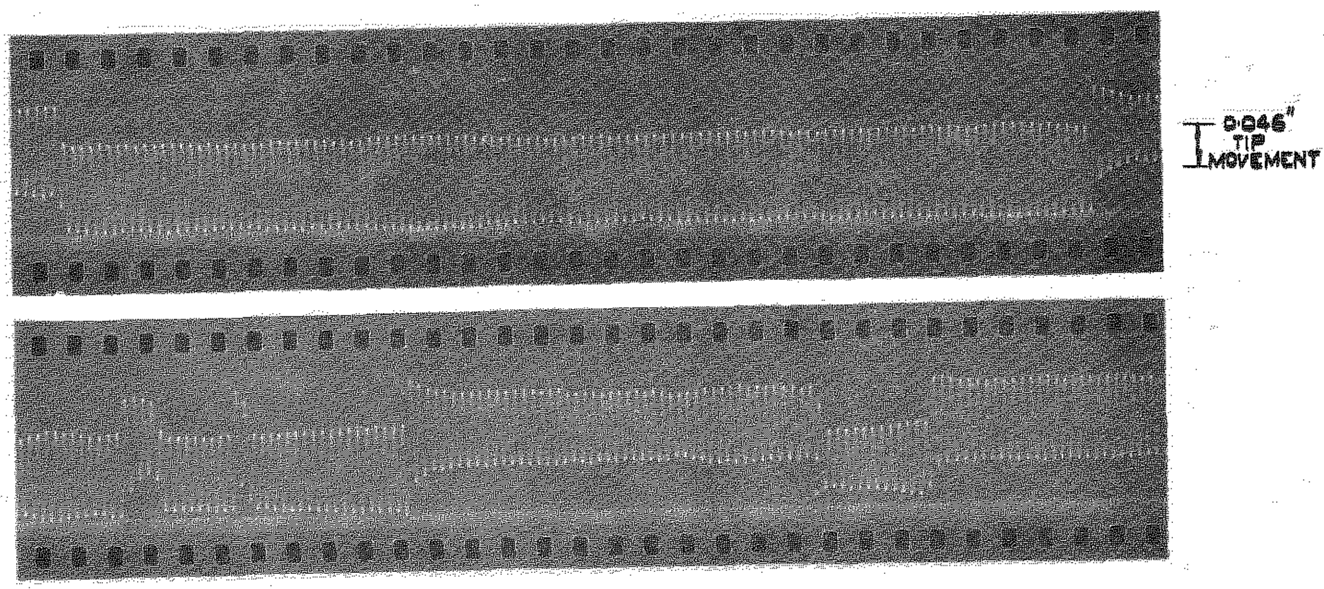

10C4/40C50 $\gamma = -34{\cdot}9^\circ$ $\alpha_1 = 62{\cdot}1^\circ$
'UNSTABLE' CONDITION, WITH FLUTTER, AT HIGH FLOW.

FLUTTER RECORDS.

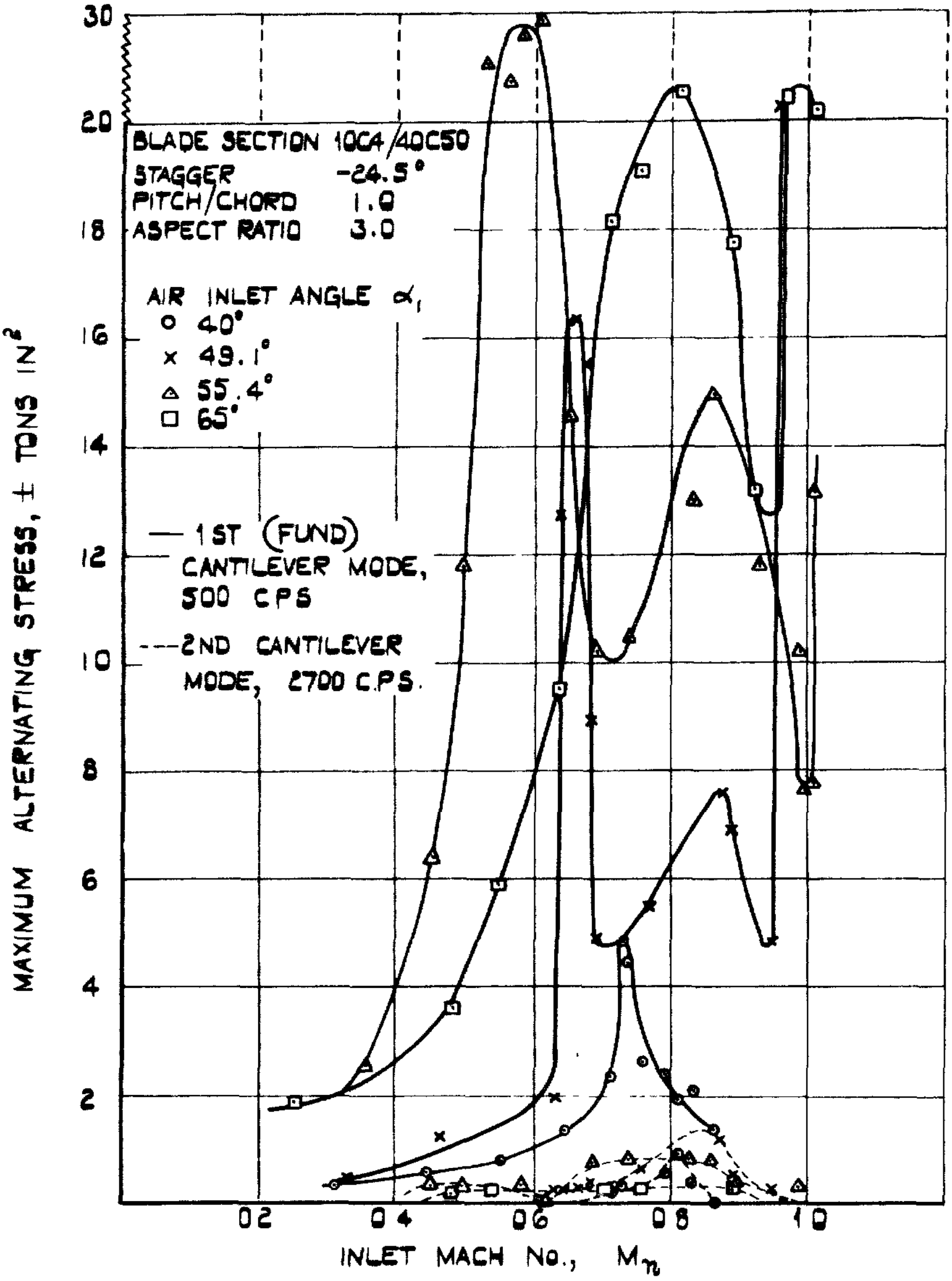

FLUTTER CHARACTERISTICS FOR LOW STAGGER (40° CAMBER) CASCADE.

FIG. 4.

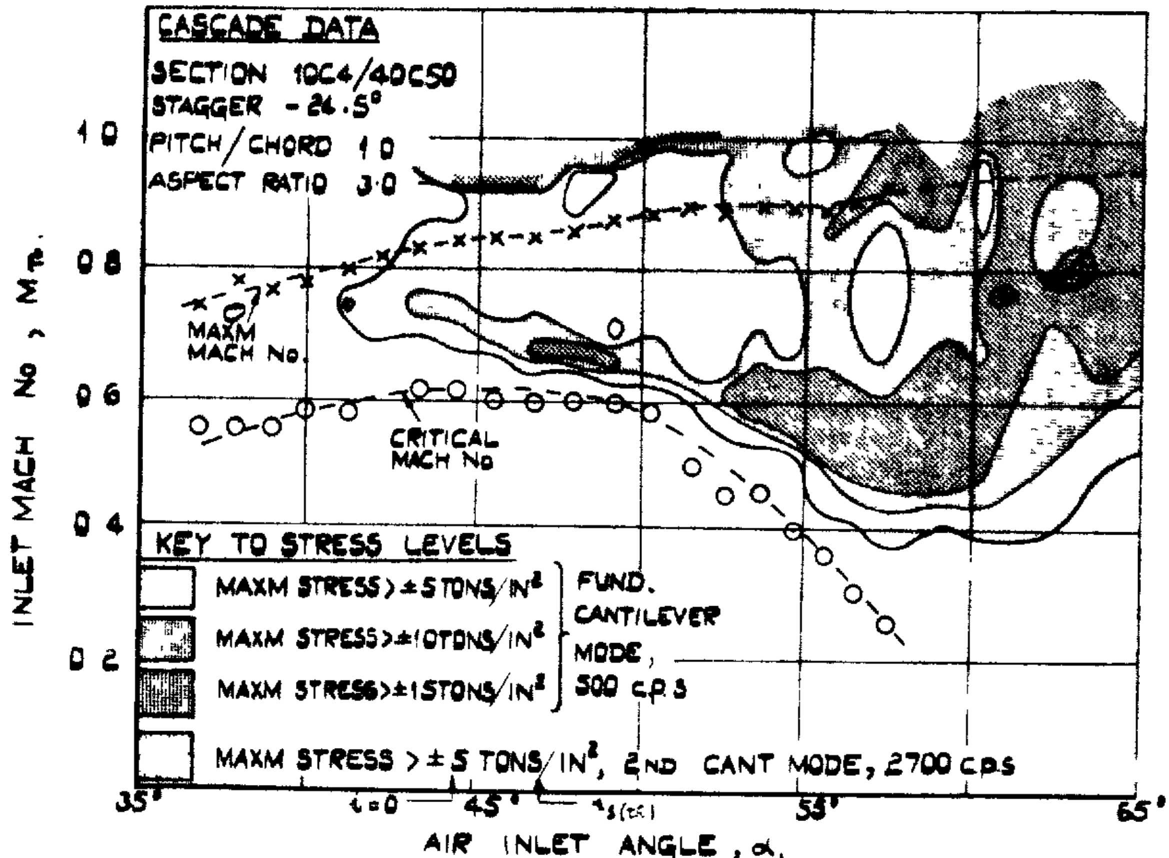

(a) MAXIMUM STRESS LEVELS

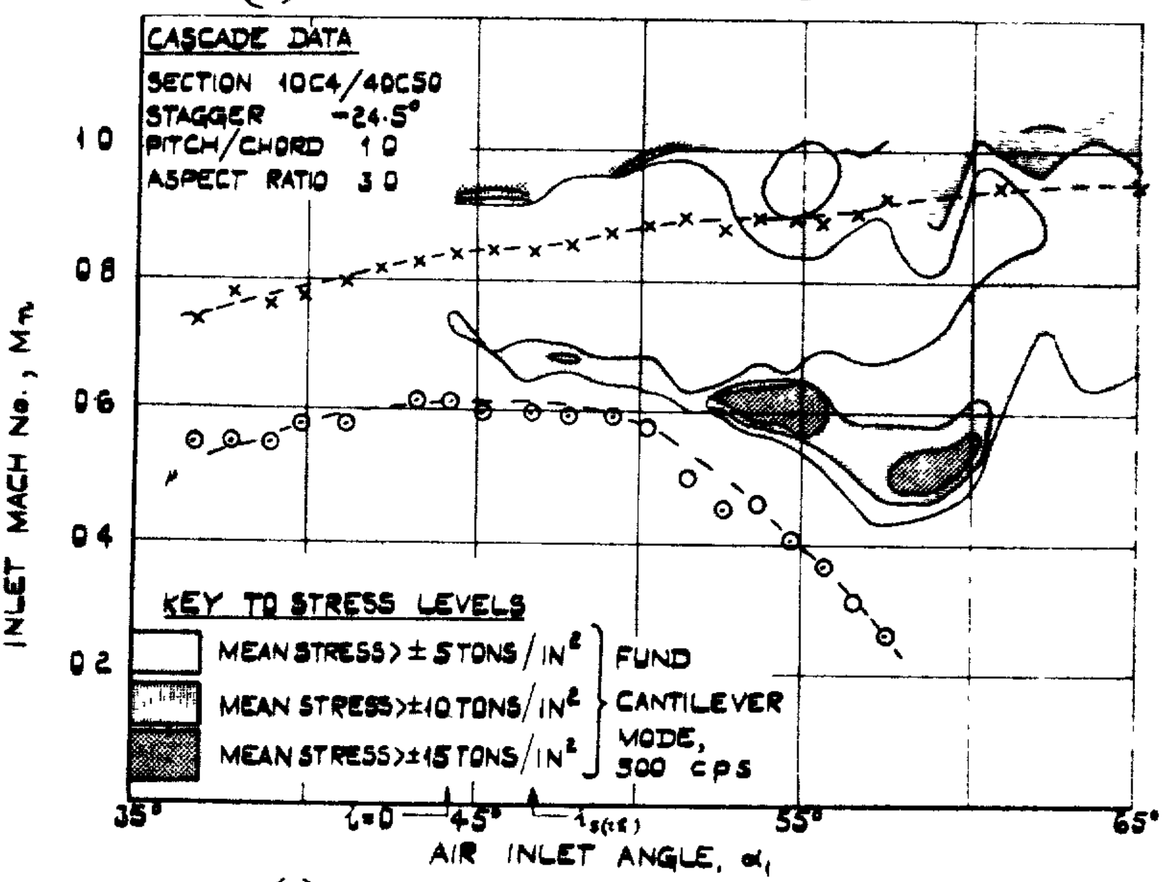

(b) MEAN STRESS LEVELS

LOCATION OF FLUTTER.
(LOW STAGGER 40° CAMBER CASCADE.)

FIG. 5.

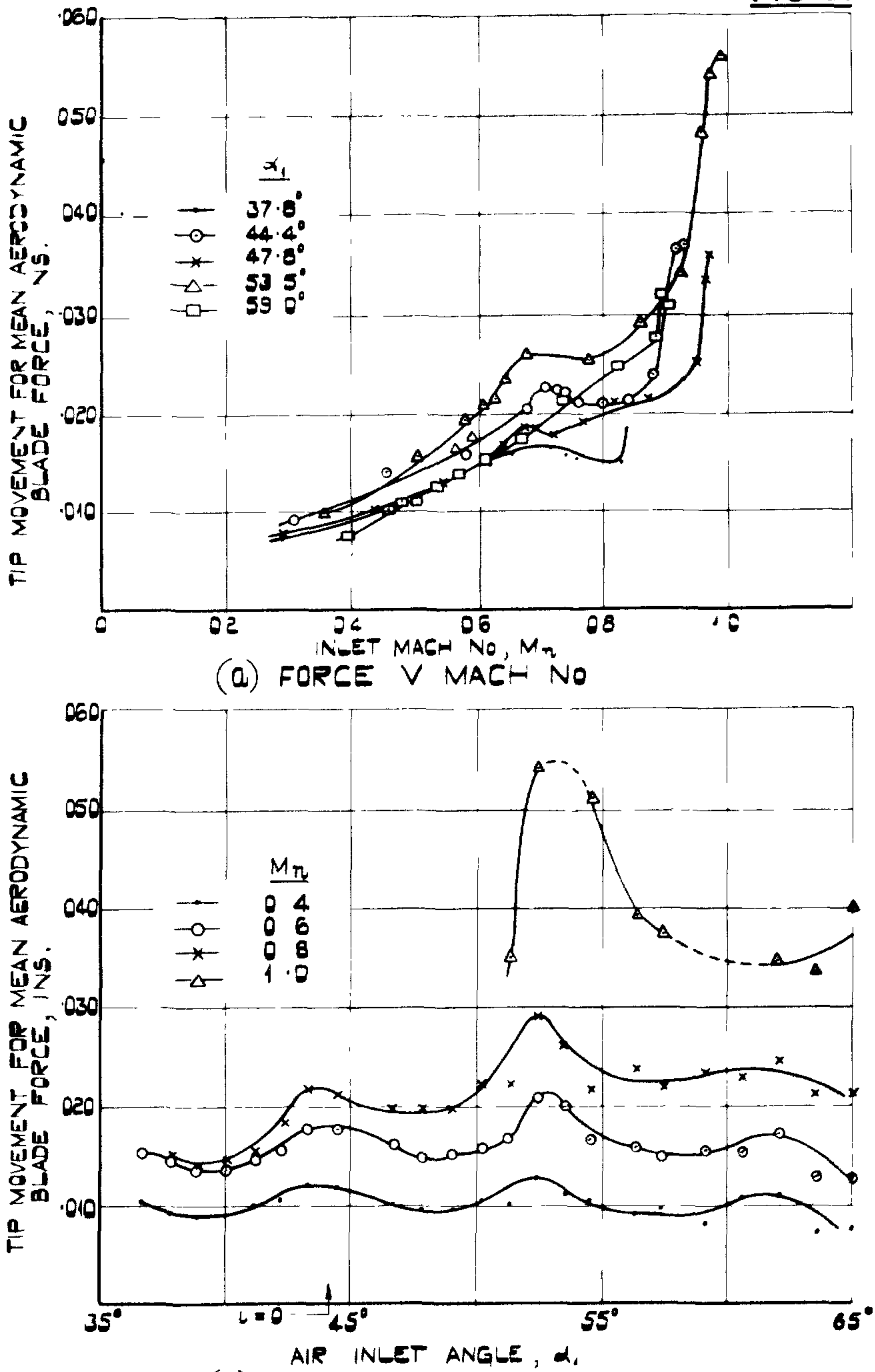

(b) FORCE V INCIDENCE

FORCE CHARACTERISTICS FOR LOW STAGGER, 40° CAMBER, CASCADE BLADE.

FIG. 6

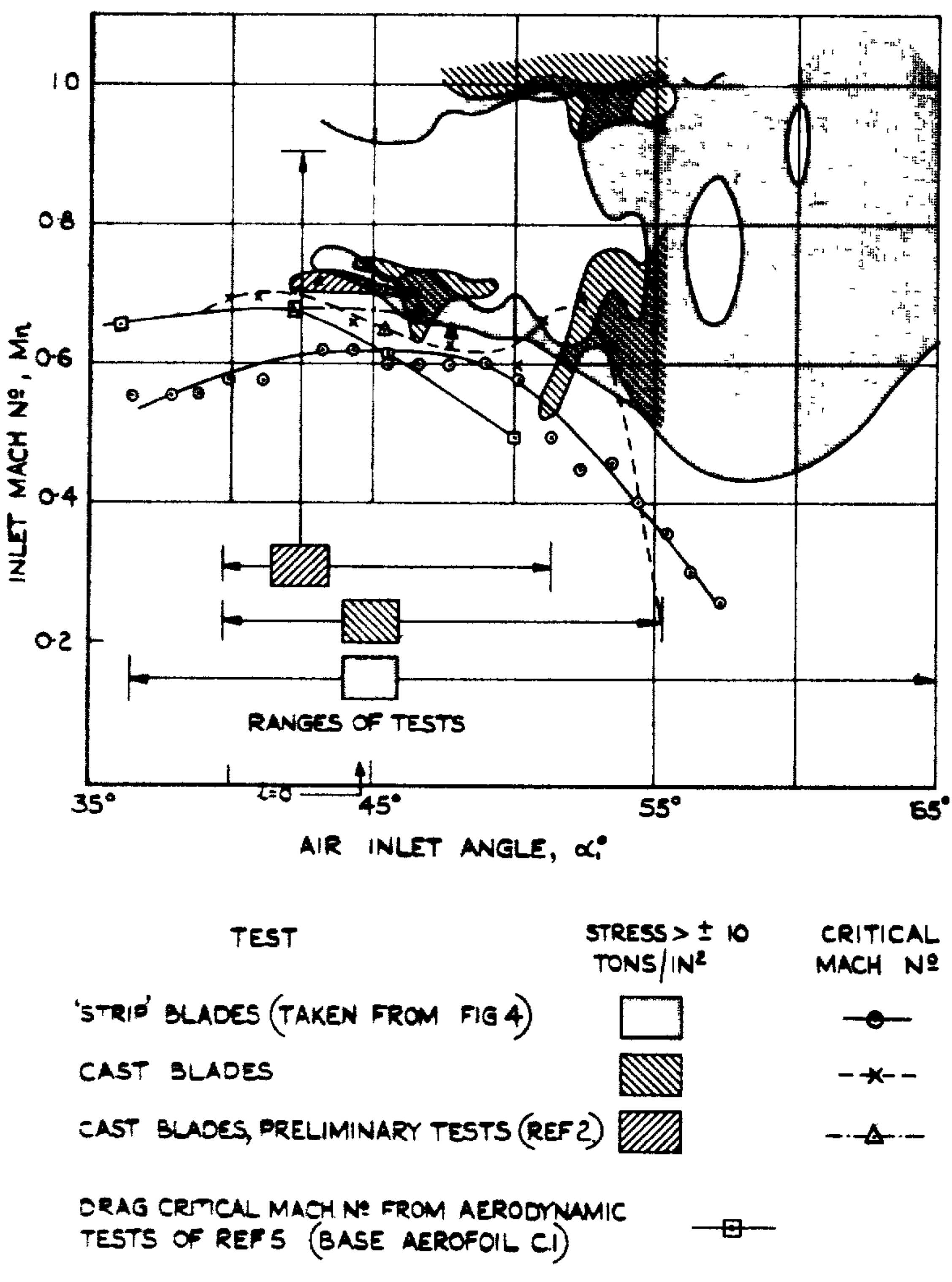

SOME COMPARATIVE RESULTS FROM LOW STAGGER 40° CAMBER CASCADES

FIG. 7

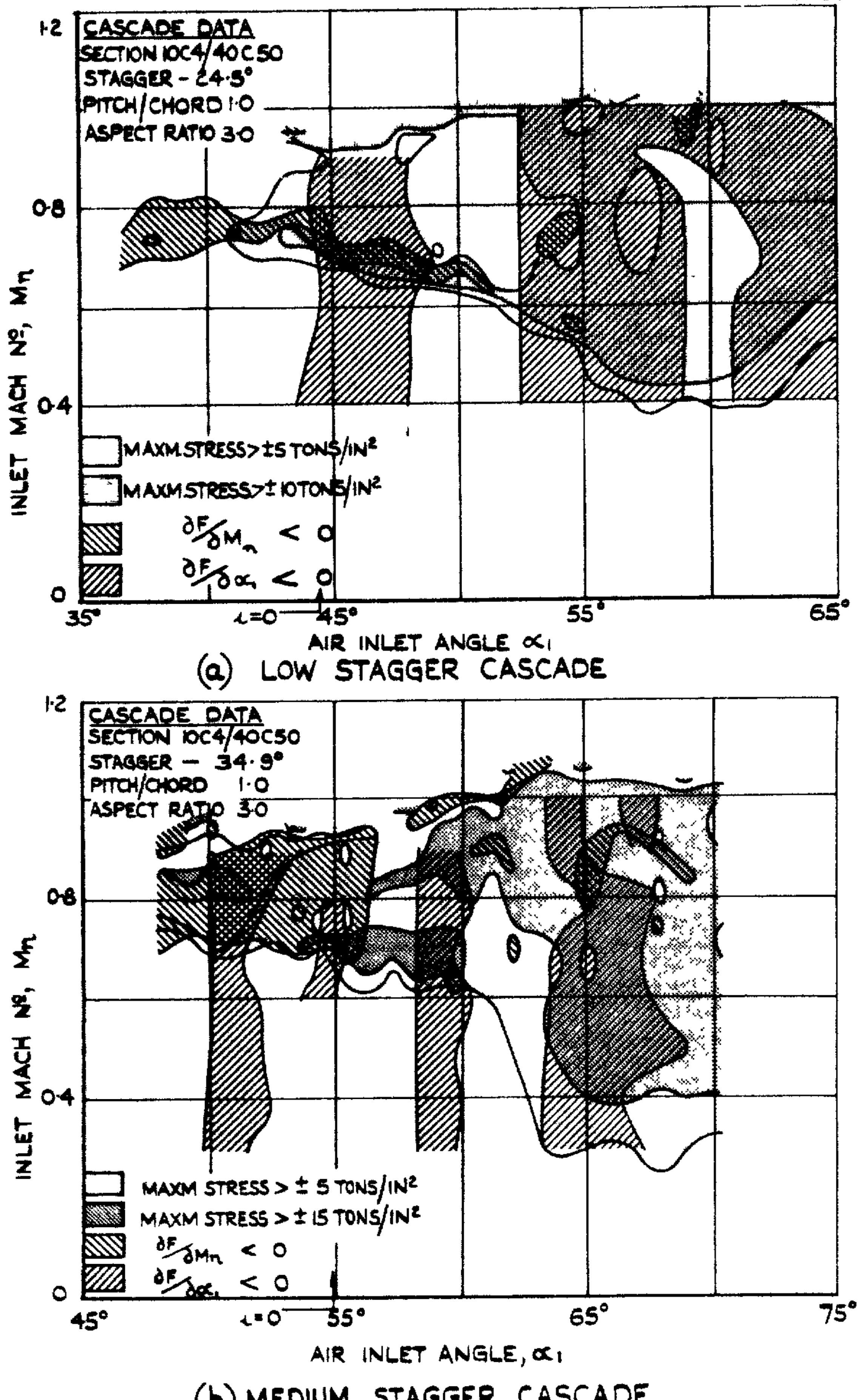

COMPARISON OF REGIONS OF NEGATIVE SLOPE OF FORCE CURVES AND FLUTTER

FIG. 8

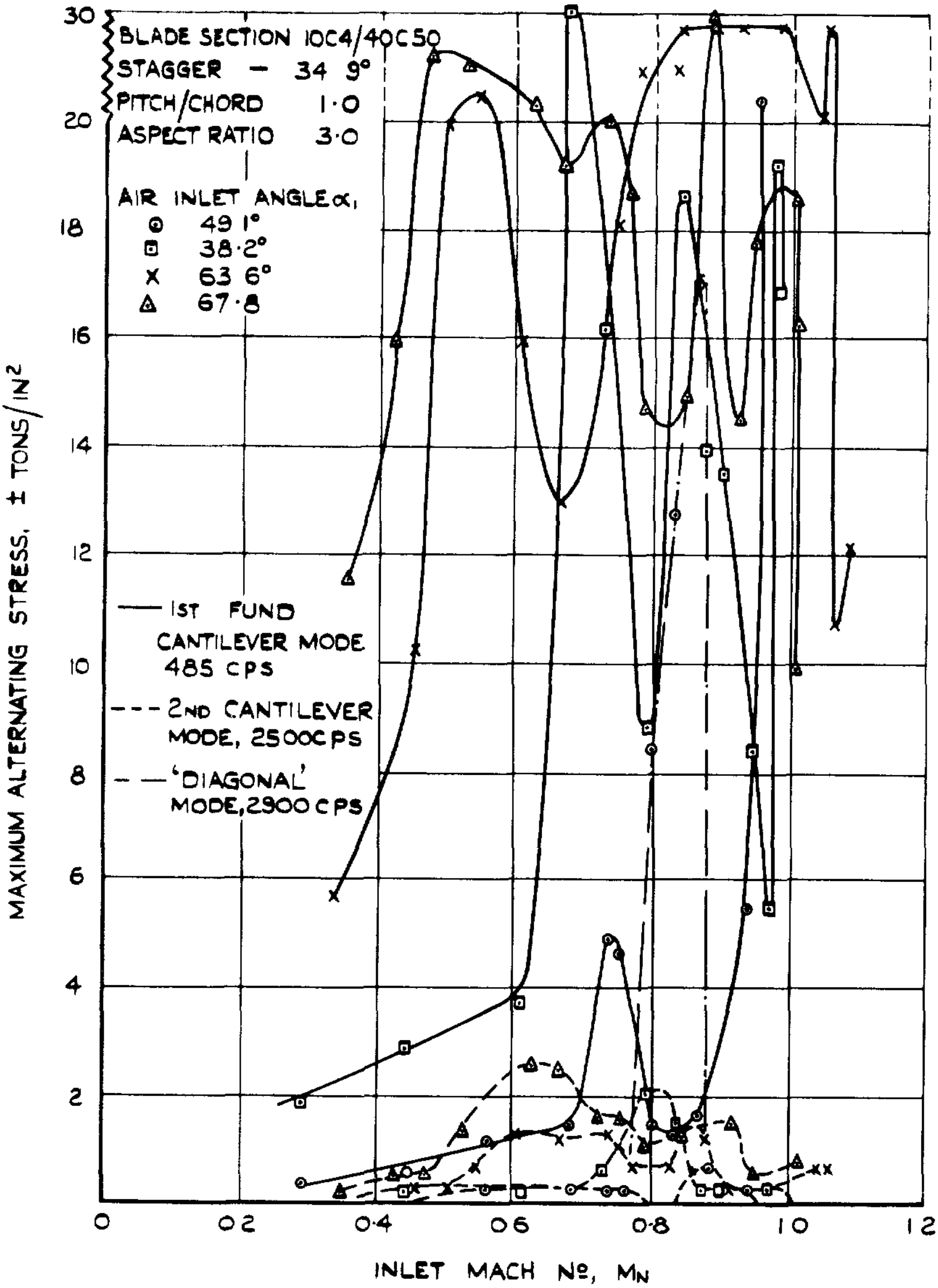

FLUTTER CHARACTERISTICS FOR MEDIUM STAGGER (40° CAMBER) CASCADE

FIG. 9

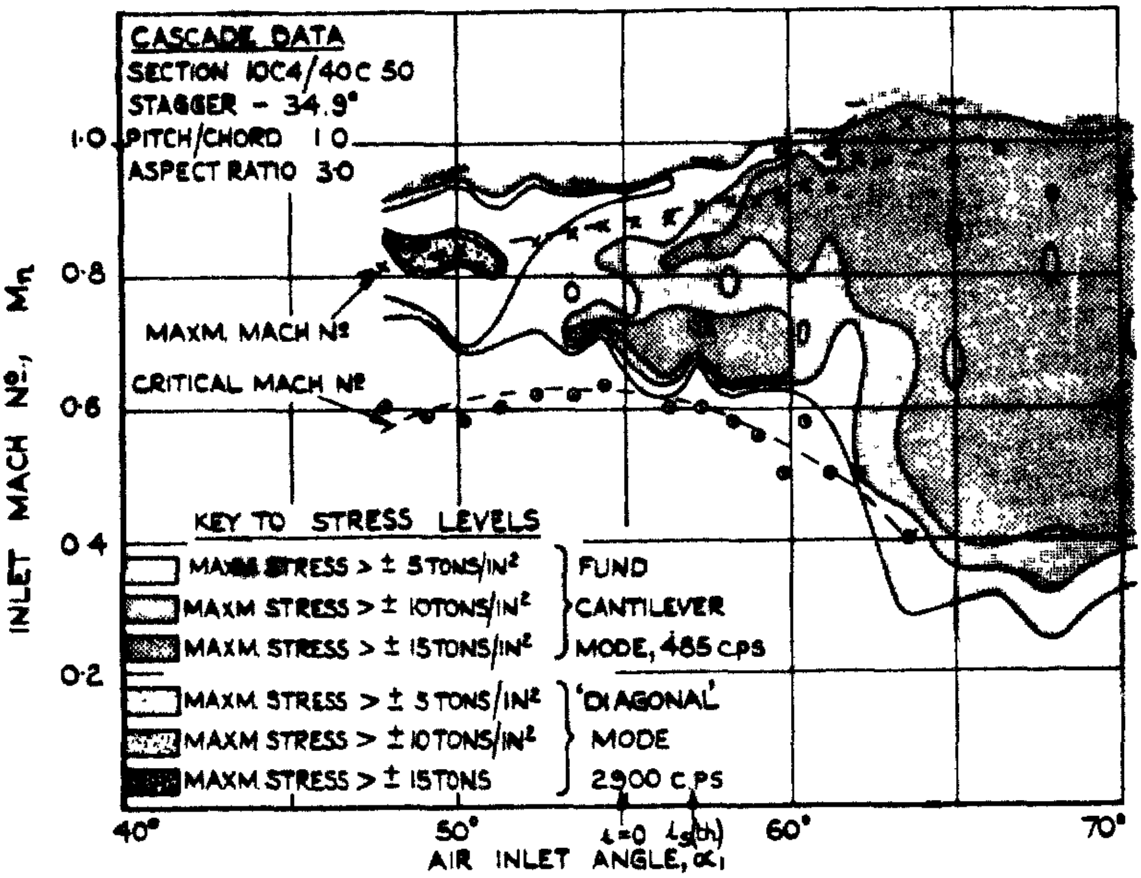

(a) MAXIMUM STRESS LEVELS

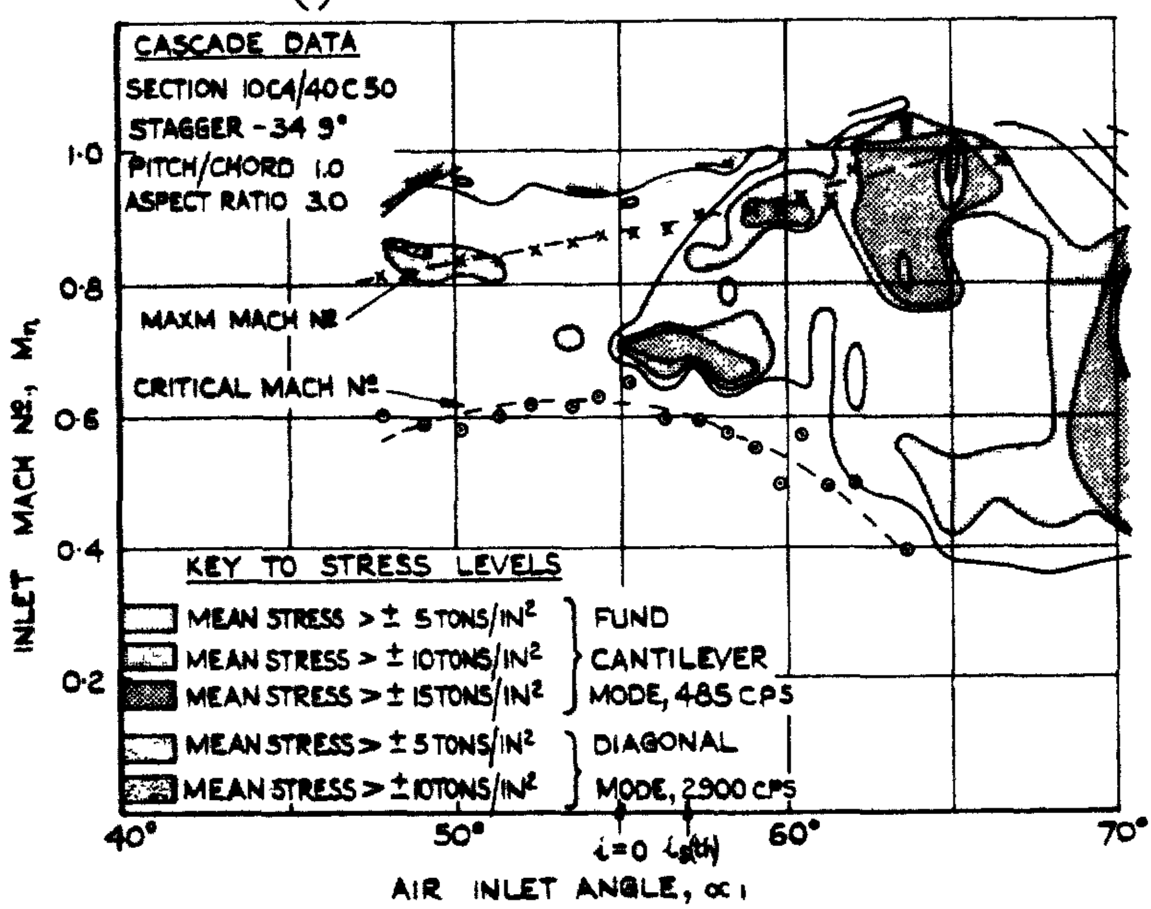

(b) MEAN STRESS LEVELS

LOCATION OF FLUTTER

MEDIUM STAGGER 40° CAMBER CASCADE

FIG. 10

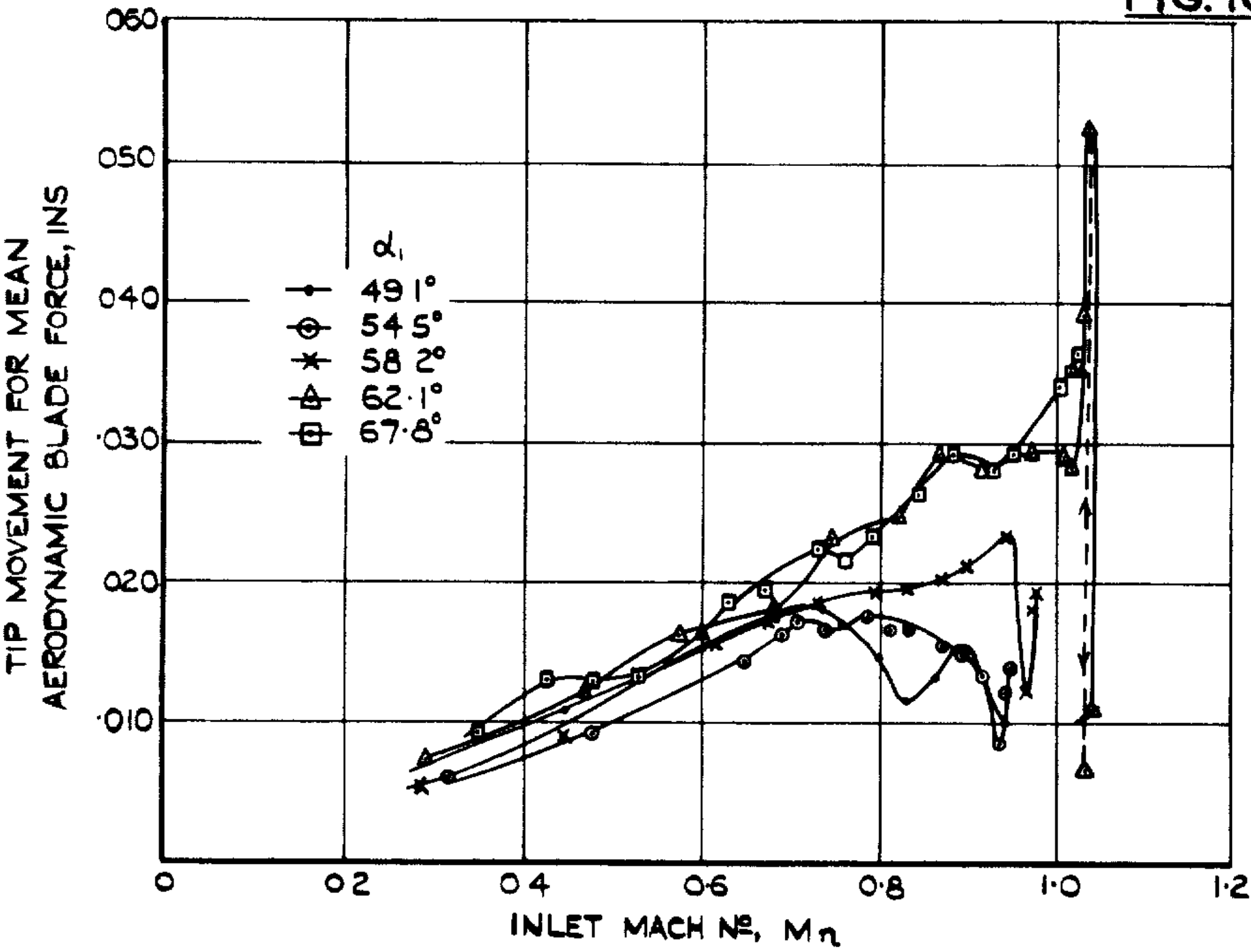

(a) FORCE v MACH No

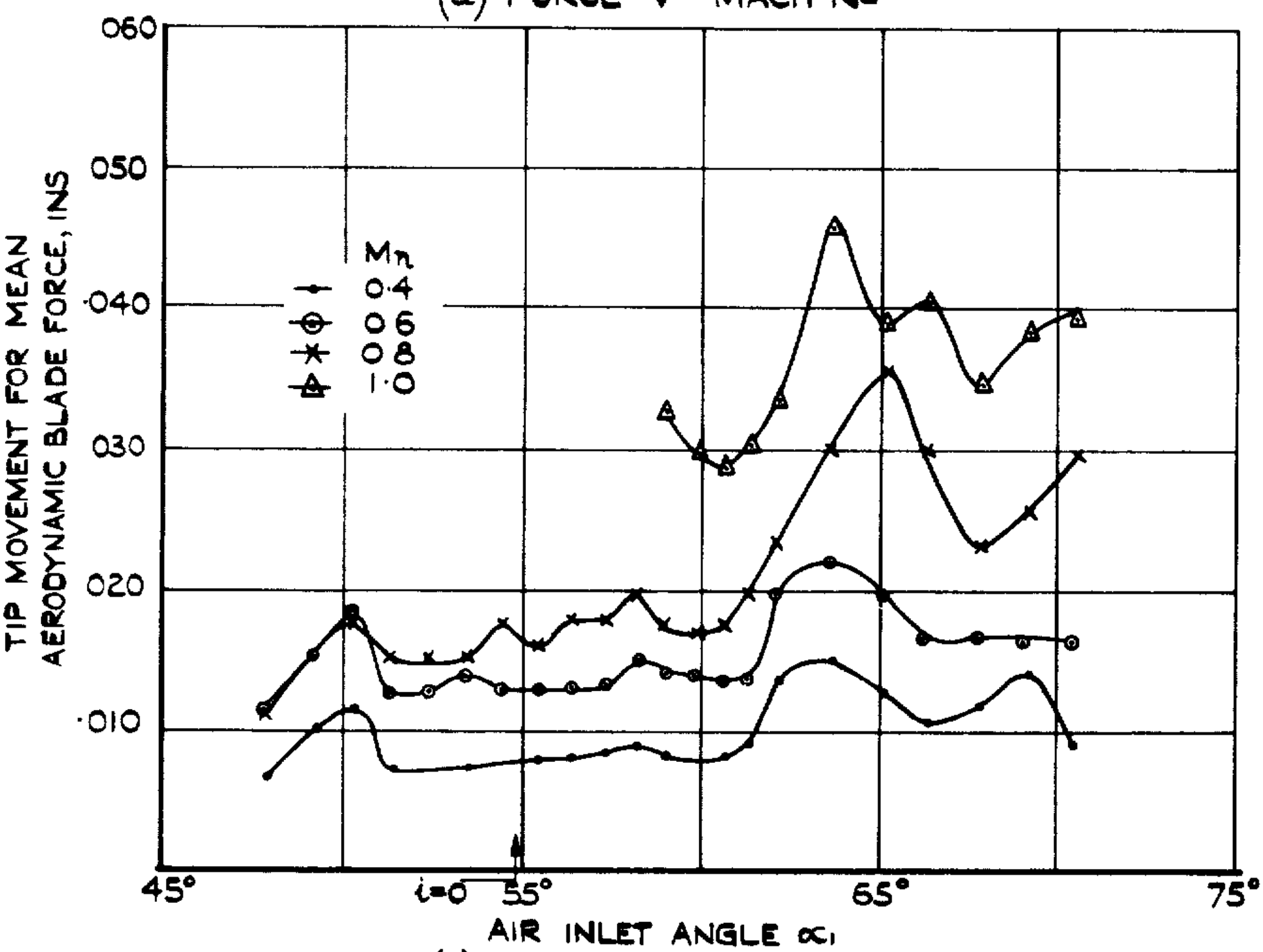

(b) FORCE v INCIDENCE.

FORCE CHARACTERISTICS FOR MEDIUM STAGGER, 40° CAMBER, CASCADE BLADE

DS 48730/1 R72 300 10/56 CL

C.P. No. 296
(17,573)

A.R.C. Technical Report

Printed and published by
HER MAJESTY'S STATIONERY OFFICE

To be purchased from
York House, Kingsway, London W.C.2
423 Oxford Street, London W.1
P.O. Box 569, London S.E.1
13A Castle Street, Edinburgh 2
109 St. Mary Street, Cardiff
39 King Street, Manchester 2
Tower Lane, Bristol 1
2 Edmund Street, Birmingham 3
80 Chichester Street, Belfast
or through any bookseller

Printed in Great Britain

S O. Code No. 23-9009-96

C.P. No. 296